Diffraction Patterns of the Millimeter Wave with a Helical Wavefront by a Triangular Aperture

Diffraction Patterns of the Millimeter Wave with a Helical Wavefront by a Triangular Aperture

Yuki. Goto · Toru. I. Tsujimura · Shin. Kubo

Abstract In this paper, for the first time, we developed the measurement method of the Topological Charge (TC) in millimeter wave with helical wavefront by a triangular aperture. The millimeter wave with helical wavefront was passively generated by conversion from a Gaussian beam using a spiral mirror, which we also developed. Each diffraction pattern depended on TC, and negative TC and positive TC were symmetric pairs under reflection. These diffraction patterns were perfectly compatible with the calculation results.

Keywords Diffraction · Vortex · Helical Wavwfront · Aperture

1 Introduction

In 1992, a Laguerre Gaussian (LG) mode known as an optical vortex is shown by Allen *et al.* [1]. It is well known that a Hermite Gaussian mode without a vortex property has a plane or spherical equiphase front, while on the other hand the equiphase front of an optical vortex has a spiral phase front. Also, it is known that an optical vortex has not only Spin Angular Momentum (SAM) characterized by the polarization of its waves but also Orbital Angular Momentum (OAM). Basically, an optical vortex is passively generated by using optical elements such as a spiral phase plate, a computer-generated hologram, and a q-plate [2][3][4]. However, it is suggested in helical undulator radiation that radiation from a charged particle in spiral motion has a helical wavefront. Studies regarding actively generated radiation with a helical wavefront without using optical elements have been started [5][6]. Recently, it has been theoretically and experimentally shown that radiation from a charged particle in spiral motion has a helical wavefront by Katoh *et al.* [7][8]. From this, it becomes possible to generate a vortex beam actively.

Yuki. Goto · Shin. Kubo
Department of Applied Energy, Nagoya University, Nagoya 464-8603, Japan,
E-mail: goto.yuki@k.mbox.nagoya-u.ac.jp

Toru. I. Tsujimura · Shin. Kubo
National Institute for Fusion Science, National Institutes of Natural Sciences, Toki 509-5292, Japan

Since the frequency of an actively generated vortex beam depends on the rotation frequency of the charged particle, it becomes possible to generate a vortex beam in any wave band. Therefore, vortex beams have been actively generated in several frequency bands such as Gamma ray, x-ray, and ultraviolet, which are high-energy vortex beams because limitation of the optical elements no longer exists [9][10][11][12][13][14][15].

With a focus on generation of a millimeter wave with helical wavefront, we have carried out an Electron Cyclotron Emission (ECE) experiment. Since electron cyclotron motion is also a type of spiral motion, ECE should also have a helical wavefront. This experiment seeks to generate high power coherent ECE with a helical wavefront [16], and then identify the Topological Charge (TC). Here, TC is also called the orbital angular momentum quantum number, which is 2π times an integer (TC) from line integrating around the optical axis. By injecting a high power Right-Handed Circular Polarized (RHCP) wave into a multi-electron system in cyclotron motion, we can generate the gyro-phase controlled multi-electron system, which can actively emit ECE with a helical wavefront. Because the radiation from an electron has a low energy, the superposition of electric fields is necessary. Although a vortex beam in millimeter wave regime has been actively investigated, studies to identify the TC of millimeter wave with helical wavefront have not been conducted. Because studies on millimeter wave with helical wavefront mainly focus on the use of the wave in telecommunication and creating vortex beams with known TC is necessary for better telecommunication [17][18][19][20][21][22][23][24]. The purpose of our research is to experimentally demonstrate the helical wavefront of actively generated ECE in millimeter wave regime by identifying the TC.

In this paper, we will show the measurement method of millimeter-wave radiation with a helical wavefront. We developed the method to estimate a helical wavefront and to identify the TC. This is a diffraction method of a millimeter wave with a helical wavefront by a triangular aperture. The beams in millimeter wave regime are low-energy beams as compared to the beams with shorter wavelength such as Gamma ray, x-ray, and ultraviolet. Using a triangular aperture with a larger area is more appropriate for our purpose than other types of aperture because more diffracted light can be obtained. This method was successfully checked by using the passively generated vortex beam from a Gaussian beam in the millimeter wave regime by a spiral mirror. The characteristic diffraction pattern of the vortex beam by a triangular aperture was observed. Since the diffraction patterns depends on the TC, we can identify the TC of the vortex beam. Actually, diffraction experiments by using several kinds of apertures outside the longer wavelength regime have been carried out, such as diffraction by single slit [25], double slits [8][26][27], triangular aperture [28][29][30][31], angular aperture [32], angular double slits [33], and off-axis diffraction by circular aperture [34]. However, a diffraction experiment in the longer wavelength regime including the millimeter wave regime has never been reported. Thus, we will report the diffraction pattern in millimeter wave with helical wavefront for the first time.

2 Experiment and Calculation Results

The diffraction experiment was carried out as shown in Fig.1. The millimeter wave with a helical wavefront was generated by conversion from a Gaussian beam from the spiral mirror [35]. Fig.2 shows a picture of the spiral mirror. The z_{m} value (height) of the spiral mirror is constant in the radial direction but varies with the azimuthal angle. Furthermore, we also developed the spiral mirror with focusing abilities. The difference of the z_{m} value at the step (at $\phi_{\mathrm{m}} = 0$) depends on the TC of the vortex beam we would like to generate, and on the injection angle. The origin of the spiral mirror has a singular point which is indefinite in z_{m} value. These spiral mirrors specialized in 45 deg. injection and reflection. We have 6 kinds of spiral mirrors with TC from -3 to +3 except for 0. The Gaussian beam with frequency 154 GHz, power 12-15 mW (measured by Mm Wave high sensitive power meter with model DPM-06 produced by ELVA-1,), and wavelength 1.95 mm was injected into the spiral mirror. Millimeter Wave Broadband BWO source with model G4-143g produced by ELVA-1 was used as the power source. The convex lens was installed between the oscillator and the spiral mirror for focusing the beam waist. The vortex beam generated by the spiral mirror was then injected into the triangular aperture, where the diffracted beam was measured by a sub-THz camera (Terahertz camera with model T30/64/64 produced by Terasense
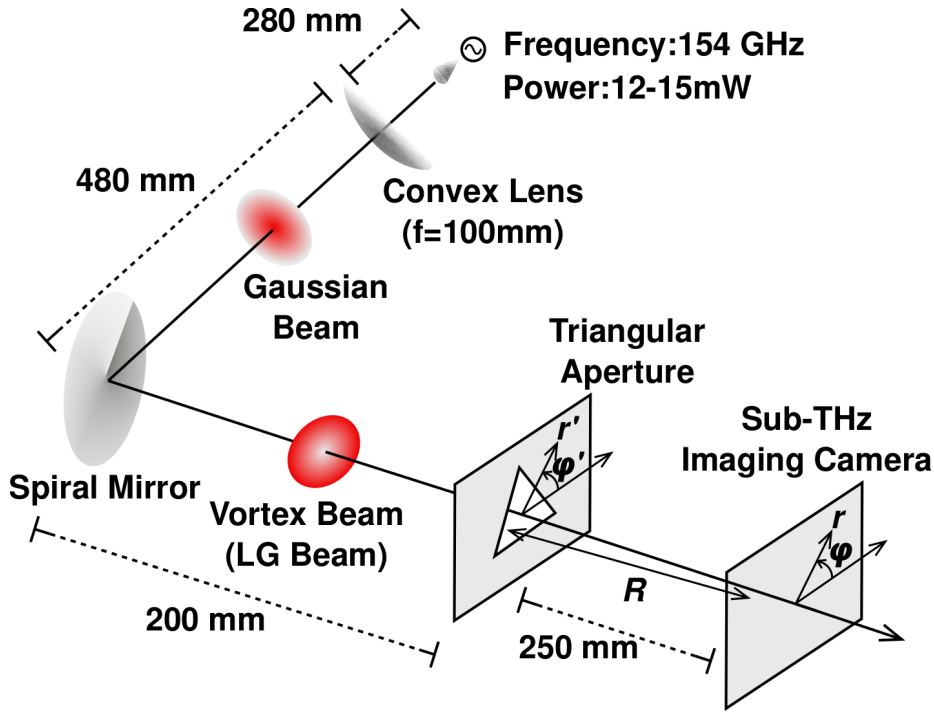

Fig. 1 Experimental setup: Sub-THz Imaging camera has sensor size 192×192 mm and 64×64 pixels, totaling 4096 pixels. The power sensitivity per pixel has 4 - 45 nW/pixel, which depends on the exposure. Frequency sensitivity also has the range from 0.02 THz (20 GHz) to 0.7 THz (700 GHz).
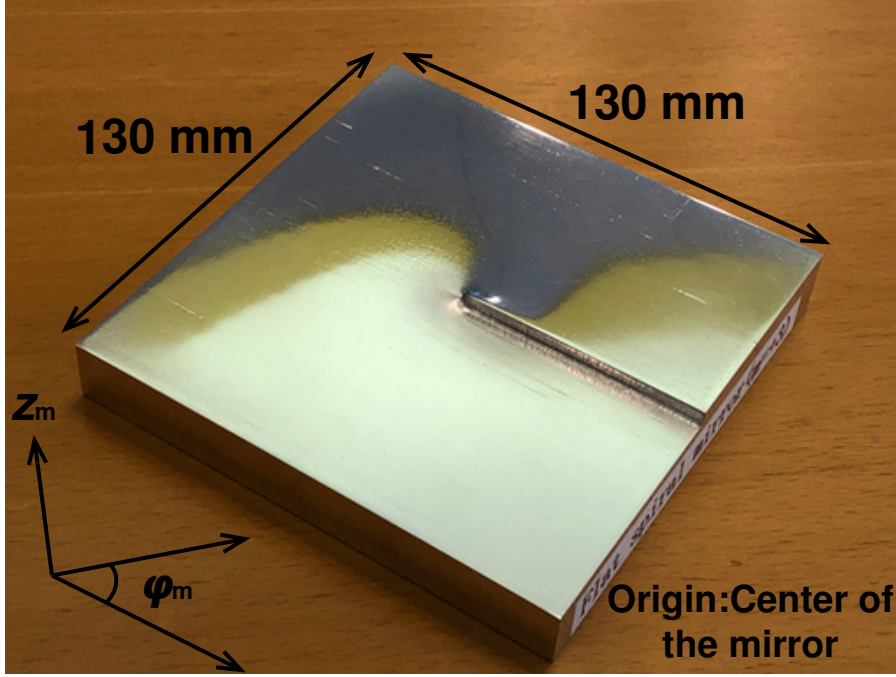
Fig. 2 Spiral mirror with TC $= +3$. The origin has a singular point with indefinite z_m value, and then the step (at $\phi_\mathrm{m} = 0$) depends on TC of the vortex beam and on the injection angle.

Group Inc.). The high-precision alignment was performed so that the optical axis and the center of gravity of the triangular aperture coincide. The distance from the oscillator to the convex lens was 280 mm, from the convex lens to the spiral mirror was 480 mm, from the spiral mirror to the aperture was 200 mm, and from the aperture to the camera was 250 mm, respectively. In the calculation, an LG beam was used for the millimeter vortex beam. An LG beam is represented as follows [1],

$$E(r, \phi, z, t) = \sqrt{\frac{2p!}{\pi(p + |l|!)}} \frac{1}{w(z)} \left(\frac{r\sqrt{2}}{w(z)}\right)^{|l|} L_p^{|l|} \left(\frac{2r^2}{w^2(z)}\right)$$

$$\times e^{\frac{-r^2}{w^2(z)}} e^{\frac{-ikr^2}{2R(z)}} e^{-i(2p+|l|+1)\tan^{-1}\left(\frac{z}{z_R}\right)} e^{-il\phi} e^{i(kz - \omega t)} \tag{1}$$

where E is the electric field; r, z, and ϕ are parameters in the cylindrical coordinate system; p and l are radius index and azimuthal index (l is equivalent to TC); L is associated Laguerre polynomials with p and l; w, k, R, and z_R are waist size, wave-number, radius of curvature, and Rayleigh length, respectively. ω and t are angular frequency and time. Diffraction by an aperture was calculated by the Huygens-Fresnel principle as follows [36],

$$D(r, \phi, z, t) = \frac{1}{4\pi} \oint_s \mathrm{d}\boldsymbol{S}' \cdot \left(\frac{\nabla' E(r', \phi', z', t')}{R} + \frac{\boldsymbol{R}}{R^3} E(r', \phi', z', t')\right.$$

$$\left. - \frac{\boldsymbol{R}}{cR^2} \frac{\partial E(r', \phi', z', t')}{\partial t'} \right)_{t' = t - \frac{R}{c}} \tag{2}$$
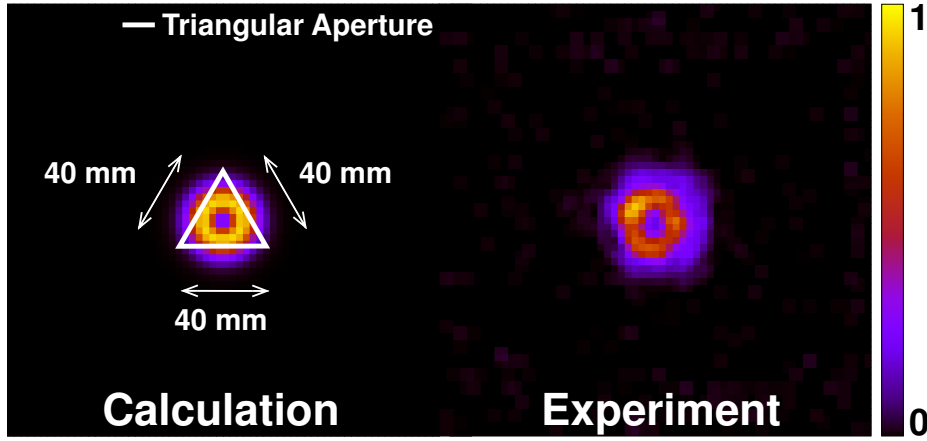
Fig. 3 Intensity distributions of the millimeter wave in 154 GHz with a helical wavefront at the aperture position. The left figure shows the calculated intensity distribution by eq.(1) with waist size 13 mm. The right figure shows the measured intensity distribution. Both figures had clear donuts-shaped intensity distribution. Scale of both the vertical axis and the horizontal axis were 200 mm, and the intensity with linear scale was normalized by being maximum value 1. Next, white line with triangle on the left figure represents size of the triangular aperture. The optical axis of the vortex beam coincided with the center of gravity of the triangular aperture, and then the bright ring was slightly larger than the inscribed circle.

where c and t' are light speed and observer time, that is, retarded time, and d$\boldsymbol{S'}$ means the integration on the aperture area. Fig.3 shows the intensity distributions with radial index $p = 0$ and azimuthal index (equivalent to TC) $l = 1$ on the aperture position. The left figure represents the calculation of the intensity distribution from an LG beam, and the right figure shows the intensity distribution of the measured result. We can see that the experimental result clearly had the donut-shaped intensity distribution which was the characteristic of the vortex beam. Here it was assumed that the calculated vortex beam had waist size of 13 mm in the light of the measured intensity distribution on the aperture position. Also the white line with triangle represents the size of the triangular aperture. As we can see, an equilateral triangular aperture with sides of 40 mm was used in this experiment. This size was large enough for the vortex beam to pass through the aperture. Actually, diffraction patterns appear more clearly if the size of the aperture is much smaller. However, in that case, most of the power of the vortex beam is cut off at the outside frame of the aperture. The power of the vortex beam before passing through the aperture was ten or more mW. But only a power of at least 10 mW can be detected by the camera. In other words, the diffraction power is larger than minimal pixel sensitivity at the pixels where the polka-dot patterns are formed if we use the power source as the LG beam with 10 mW. Note that this value completely depends on the experimental setup, especially the aperture size, beam size on the aperture position, and pixel sensitivity. Note that this value totally depends on the experimental setup, especially the aperture size, beam size on the aperture position, pixel sensitivity. Therefore, we set the sides of the aperture to 40 mm, which allowed the power to pass through sufficiently.

Fig.4 shows the diffraction patterns by a triangular aperture of a millimeter wave with a helical wavefront. Fig.4(a) shows the case of negative TC, which is
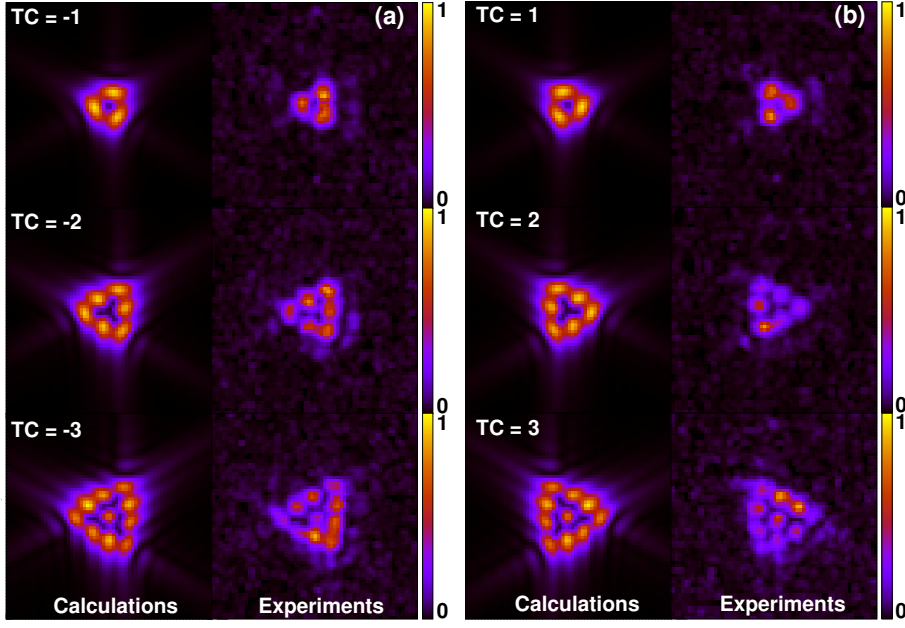
Fig. 4 (a): Diffraction patterns by the millimeter wave with a helical wavefront with negative TC. The left row is the calculation results. The right row is the experimental results. Top figures show TC = −1, middle figures show the TC = −2, and bottom figures show TC = −3. Scale of both the vertical axis and the horizontal axis are 200 mm, and then the intensity is normalized by being maximum value 1. (b): Same as Fig. 4(a), but the sign of the TC is positive.

-1, -2, and -3 from top to bottom. Fig.4(b) shows the case of positive TC, which is 1, 2, and 3 from top to bottom. In both figures, the left column represents the calculation results and the right column represents the experimental results. For generating several kinds of vortex beams, we had to replace the spiral mirror every time. Since it was an important factor that the center of gravity of the aperture coincides with the optical axis of the vortex beam, precise alignment had to be carried out every time. In the experiment, we obtained the characteristic diffraction patterns which were resemble polka-dot patterns. The diffraction patterns were also calculated by the Huygens-Fresnel principle in eq.(2). These calculation results were perfectly compatible with the experimental results. Also, as you can see, these diffraction patterns depended on TC, and negative TC and positive TC were symmetric pairs under reflection. Note that the diffraction powers measured far from the polka-dot patterns indicate the noise level. Therefore, we were able to estimate the vortex property and identify the TC even in the millimeter wave regime.

Finally, fig.5 shows the diffraction patterns by a triangular aperture of a millimeter wave without a vortex property, that is, only a Gaussian beam. As we can see, the characteristic diffraction patterns did not appear when the injected beam had no vortex property. This result is also important for identifying between a
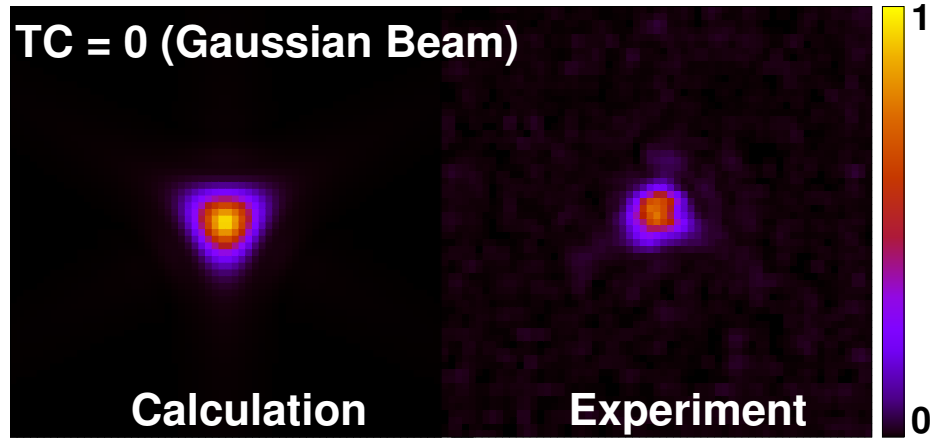
Fig. 5 Diffraction patterns by the Gaussian millimeter wave (this is equivalent to TC = 0). The left is the calculation result. The right is the experimental result. In the case of Gaussian beam, the characteristic diffraction pattern did not appear.

vortex beam and a Gaussian beam.

3 Summary

In this research, we carried out a diffraction experiment by a triangular aperture using passively generated millimeter waves with a helical wavefront, using a spiral mirror. In the experiment, donut-shaped intensity distribution was measured at the aperture position. Based on this intensity distribution, diffraction patterns were calculated using the Huygens-Fresnel principle, which had characteristic diffraction patterns that were resemble polka-dot patterns. In the experiment, the same pattern was measured. It became obvious that these diffraction patterns depend on the TC, and that negative TC and positive TC had reflection symmetry. Therefore, we were able to estimate a millimeter wave with a helical wavefront and to identify the TC. In the future, we will adapt this diffraction method by a triangular aperture to a measurement of actively generated ECE. Then we will experimentally demonstrate the vortex property of ECE.

Acknowledgments

References

1. L. Allen, M. W. Beijersbergen, R. J. C. Spreeuw, and J. P. Woerdman, "Orbital angular momentum of light and the transformation of Laguerre-Gaussiean laser modes," Phys. Rev. A, **45**, 8185 (1992).
2. J. Courtial and K. O'Holleran, "Experiments with twisted light," Eur. Phys. J. Special Topics **145**, 35-47 (2007).
3. L. Marrucci, C. Manzo, and D. Paparo, "Optical Spin-to-Orbital Angular Momentum Conversion in Inhomogeneous Anisotropic Media," Phys. Rev. Lett., **96**, 163905 (2006).
4. S. F. Busch, J. C. Balzer, G. Bastian, G. E. Town, and M. Koch, "Extending the Alvarez-Lens Concept to Arbitrary Optical Devices: Tunable Gratings, Lenses, and Spiral Phase Plates," IEEE Trans. Terahertz Sci. Technol., **7**, 3, 320-325, (2017).
5. S. Sasaki and I. McNulty, "Proposal for Generating Brilliant X-Ray Beams Carrying Orbital Angular Momentum," Phys. Rev. Lett., **100**, 124801 (2008).
6. J. Bahrdt, K. Holdack, P. Kuske, R. Muller, M. Scheer, and P. Schmid, "First Observation of Photons Carrying Orbital Angular Momentum in Undulator Radiation," Phys. Rev. Lett., **111**, 034801 (2013).
7. M. Katoh, M. Fujimoto, H. Kawaguchi, K. Tsuchiya, K. Ohmi, T. Kaneyasu, Y. Taira, M. Hosaka, A. Mochihashi, and Y. Takashima, "Angular Momentum of Twisted Radiation from an Electron in Spiral Motion," Phys. Rev. Lett., **118**, 094801 (2017).
8. M. Katoh, M. Fujimoto, N. S. Mirian, T. Konomi, Y. Taira, T. Kaneyasu, M. Hosaka, N. Yamamoto, A. Mochihashi, Y. Takahashi, K. Kuroda, A. Miyamoto, K. Miyamoto, and S. Sasaki, "Helical Phase Structure of Radiation from an Electron in Circular Motion," Sci. Rep., **7**, 6130 (2017).
9. Y. Taira, T. Hayakawa, and M. Katoh, "Gamma-ray vortices from nonlinear inverse Thomson scattering of circularly polarized light," Sci. Rep., **7**, 5018 (2017).
10. Y. Taira and M. Katoh, "Generation of Optical Vortices by Nonlinear Inverse Thomson Scattering at Arbitrary Angle Interactions," Astrophys. J., **860**, 11 (2018).
11. T. Maruyama, T. Hayakawa, and T. Kajino, "Compton Scattering of γ-Ray Vortex with Laguerre Gaussian Wave Function," Sci. Rep., **9**, 51 (2019).
12. S. Matsuba, K. Kawase, A. Miyamoto, S. Sasaki, M. Fujimoto, T. Konomi, N. Yamamoto, M. Hosaka, and M. Katoh, "Generation of vector beam with tandem helical undulators," Appl. Phys. Lett., **113**, 021106 (2018).
13. T. Kaneyasu, Y. Hikosaka, M. Fujimoto, T. Konomi, M. Katoh, H. Iwayama, and E. Shigemasa, "Limitations in photoionization of helium by an extreme ultraviolet optical vortex," Phys. Rev. A, **95**, 023413, (2017).
14. Y. Taira and M. Katoh, "Gamma-ray vortices emitted from nonlinear inverse Thomson scattering of a two-wavelength laser beam," Phys. Rev. A, **98**, 052130, (2018).
15. T. Kaneyasu, Y. Hikosaka, M. Fujimoto, H. Iwayama, M. Hosaka, E. Shigemasa, and M. Katoh, "Observation of an optical vortex beam from a helical undulator in the XUV region," J. Synchrotron Rad., **24**, 934-938, (2017).
16. Y. Goto, T. I. Tsujimura, and S. Kubo, "Development of the Grating Mirror for the High Power Transmission System and Its General Theory," Plasma Fusion Res., **13**, 3405089 (2018).
17. Y. Yan, G. Xie, M. P.J. Lavery, H. Huang, N. Ahmed, C. Bao, Y. Ren, Y. Cao, L. Li, Z. Zhao, A. F. Molisch, M. Tur, M. J. Padgett, and A. E. Willner, "High-capacity millimetre-wave communications with orbital angular momentum multiplexing," Nat. Commun., **5**, 4876, (2014).
18. N. Bozinovic, Y. Yue, Y. Ren, M. Tur, P. Kristensen, H. Huang, A. E. Willner, and S. Ramachandran, "Terabit-Scale Orbital Angular Momentum Mode Division Multiplexing in Fibers," Science, **340**, 4876, (2013).
19. X. Hui, S. Zheng, Y. Chen, Y. Hu, X. Jin, H. Chi, and X. Zhang, "Multiplexed Millimeter Wave Communication with Dual Orbital Angular Momentum (OAM) Mode Antennas," Sci. Rep., **5**, 10148, (2015).
20. S. Yu, L. Li, and G. Shi, "Dual-polarization and dual-mode orbital angular momentum radio vortex beam generated by using reflective metasurface," Appl. Phys. Express, **9**, 082202, (2016).
21. S. Yu, L. Li, G. Shi, C. Zhu, and Y. Shi, "Generating multiple orbital angular momentum vortex beams using a metasurface in radio frequency domain," Appl. Phys. Lett., **108**, 241901, (2016).

22. H. Wu, J. Tang, Z. Yu, J. Yi, S. Chen, J. Xiao, C. Zhao, Y. Li, L. Chena, and S. Wen, "Electrically optical phase controlling for millimeter wave orbital angular momentum multimodulation communication," Opt. Commun., **393**, 49-55 (2017).
23. F. Tamburini, E. Mari, B. Thidé, C. Barbieri, and F. Romanato, "Experimental verification of photon angular momentum and vorticity with radio techniques," Appl. Phys. Express, **99**, 204102, (2011).
24. A, E. Willner, Y. Ren, G. Xie, Y. Yan, L. Li, Z. Zhao, J. Wang, M. Tur, A. F. Molisch, and S. Ashrafi, "Recent advances in high-capacity free-space optical and radio-frequency communications using orbital angular momentum multiplexing," Phil. Trans. R. Soc. A, **375**, 20150439, (2017).
25. D. P. Ghai, P. Senthilkumaran, and R. Sirohi, "Single-slit diffraction of an optical beam with phase singularity," Optics and Lasers in Engg., **47**, vol. 1, 123-126, (2009).
26. S. Zheng and J. Wang, "Measuring Orbital Angular Momentum (OAM) States of Vortex Beams with Annular Gratings," Sci. Rep., **7**, 40781 (2017).
27. H. I. Sztul and R. R. Alfano, "Double-slit interference with Laguerre–Gaussian beams," Opt. Lett., **31**, 31, (2006).
28. L. E. E. de Araujo and M. E. Anderson, "Measuring vortex charge with a triangular aperture," Opt. Lett., **36**, 36, (2011).
29. J. M. Hickmann, E. J. S. Fonseca, W. C. Soares, and S. Chavez-Cerda, "Unveiling a Truncated Optical Lattice Associated with a Triangular Aperture Using Light ' s Orbital Angular Momentum," Phys. Rev. Lett., **105**, 053904 (2016).
30. A. Mourka, J. Baumgartl, C. Shanor, K. Dholakia, and E. M. Wright, "Visualization of the birth of an optical vortex using diffraction from a triangular aperture," Opt. Express, **19**, 7, (2011).
31. Y. Taira and Y. Kohmura, "Measuring the topological charge of an x-ray vortex using a triangular aperture.pdf," J. Opt., **21**, 045604, (2019).
32. C. S. Guo, L. L. Lu, and H. T. Wang, "Characterizing topological charge of optical vortices by using an annular aperture," Opt. Lett., **34**, 23, (2009).
33. D. Fu, D. Chen, R. Liu, Y. Wang, H. Gao, F. Li, and P. Zhang, "Probing the topological charge of a vortex beam with dynamic angular double slits," Opt. Lett., **40**, 5, (2015).
34. Y. Taira and S. Zhang, "Split in phase singularities of an optical vortex by off-axis diffraction through a simple circular aperture," Opt. Lett., **42**, 7, (2017).
35. D. P. Ghai, P. Senthilkumaran, and R. Sirohi, "Adaptive helical mirror for generation of optical phase singularity," Appl. Opt., **47**, 10, 1378-1383, (2008).
36. S. Sunakawa, "Riron Denjikigaku" 3rd ed. [in Japanese] (Theoretical Electromagnetism), Kinokuniya, Tokyo, (2010).